



HAL
open science

Antimicrobial peptide arrays for wide spectrum sensing of pathogenic bacteria

Éric Pardoux, Agnès Roux, Raphaël Mathey, Didier Boturyn, Yoann Roupioz

► **To cite this version:**

Éric Pardoux, Agnès Roux, Raphaël Mathey, Didier Boturyn, Yoann Roupioz. Antimicrobial peptide arrays for wide spectrum sensing of pathogenic bacteria. *Talanta*, 2019, 203, pp.322-327. 10.1016/j.talanta.2019.05.062 . hal-02565818

HAL Id: hal-02565818

<https://hal.science/hal-02565818>

Submitted on 23 Sep 2020

HAL is a multi-disciplinary open access archive for the deposit and dissemination of scientific research documents, whether they are published or not. The documents may come from teaching and research institutions in France or abroad, or from public or private research centers.

L'archive ouverte pluridisciplinaire **HAL**, est destinée au dépôt et à la diffusion de documents scientifiques de niveau recherche, publiés ou non, émanant des établissements d'enseignement et de recherche français ou étrangers, des laboratoires publics ou privés.

Antimicrobial peptide arrays for wide spectrum sensing of pathogenic bacteria

Éric Pardoux^{a,b}, Agnès Roux^a, Raphaël Mathey^a, Didier Boturyn^b, Yoann Roupioz^{a,*}

^aUniv. Grenoble Alpes, CNRS, CEA, INAC-SyMMES, 38000 Grenoble, France

^bUniv. Grenoble Alpes, CNRS, DCM, 38000 Grenoble, France

*Corresponding author: yoann.roupioz@cea.fr

Abstract

Fast detection of bacteria in samples presumed to be un-contaminated, such as blood, is of great importance. Indeed, rapid diagnosis allows the set-up of appropriate antibiotic treatment. Besides clinical issues, there are many other domains, such as food processing or drug manufacturing, where the strict absence of any bacteria has to be assessed. Because the bacterial load found in most contaminated samples is often below the limit of detection for currently validated assays, a preliminary enrichment step is required to allow bacterial multiplication before proceeding to the analysis step, whatever it might be – cultural, immunological or molecular methods. In this study, we describe the use of a biosensor for single-step bacteria detection. The whole analysis is performed in less than 20 hours, during the growth phase of the micro-organisms, using an array of antimicrobial peptides (AMPs) coupled with a surface plasmon resonance imager (SPRI). A wide range of bacterial strains are assayed, showing differentiated affinity patterns with the immobilized peptides, which are confirmed by multivariate analysis. This work establishes the evidence that antimicrobial peptides, mostly used so far in the antibiotic drug industry, are suited for the wide-spectrum detection of unknown bacteria in samples, even at very low initial loads. Moreover, the small set of AMPs that were assayed provided a specific affinity profile for each pathogen, as confirmed by multivariate analyses. Furthermore, this work opens up the possibility of applying this method in more complex and relevant samples such as foodstuff, urine or blood.

Keywords

Antimicrobial Peptides; Bacteria Detection; Pathogens; Surface Plasmon Resonance imaging

33 Introduction

34 The presence of bacteria in a normally sterile environment is a huge issue for human health,
35 since it can cause severe infections. Whether they originate in foodstuffs or bodily fluids such as
36 blood or urine, the rapid and sensitive detection of pathogenic microorganisms is thus of great
37 importance. Although fast diagnosis is vital during an infection, the early detection of pathogens
38 is made difficult because of their low concentrations. For this reason, all samples drawn from
39 patients are first diluted and cultured in a liquid medium to increase the bacterial concentration,
40 before proceeding to the analysis of the enriched samples. So far, culture-based techniques
41 have remained the gold standard in the process of diagnosing bacterial infections, though
42 several alternative methods have emerged in recent decades to devise faster and more
43 sensitive ways to achieve bacterial detection [1]. Assays based on DNA amplification have
44 paved their way to a large use in clinics [2]. In spite of their faster response, these assays are
45 still time-consuming, quite expensive, and require a high level of skills. Moreover, such methods
46 may give false-positive results due to the presence of residual DNA, released from killed
47 pathogenic bacteria in some samples, for instance after antibiotic treatment. Mass spectrometry
48 has also become widely used for the precise identification of strains [3]. However, it requires
49 isolated colonies of the pathogen to be grown on a solid medium and thus can only be
50 performed several days after enrichment of the sample. Owing to these considerations, new
51 technologies enabling faster diagnostics are still emerging, promising simple and low-cost on-
52 field implementation [4,5]. Amongst other alternatives under research, biosensors able to detect
53 whole viable cells directly from a suspect sample are very promising. Nevertheless, each of
54 these exciting alternatives still require a preliminary enrichment step to increase the initial
55 bacterial concentration above their limit of detection (10^3 to 10^6 CFU.ml⁻¹, depending on the
56 method). Surprisingly, only a few approaches couple the enrichment step with the detection
57 step. From this perspective, surface plasmon resonance imaging (SPRI) is a promising method.
58 Indeed, this technique is based on the optical detection of interactions at the surface of a
59 metallic layer, thus enabling the monitoring of molecular interactions without labels. Although
60 SPRI-based molecular detections are less sensitive than ELISA for biomolecular interaction
61 studies, SPRI has been used in versatile applications from molecular studies to whole cell or
62 living bacteria detection, taking advantage of its real-time and label-free multiplexing abilities
63 [6,7]. This optical method has already proven its ability to successfully detect and identify
64 pathogens starting from food matrices or blood spiked with low bacterial concentrations (few
65 CFU.ml⁻¹), using arrays of proteins and antibodies [8–11]. Such one-step approach enables
66 sensitive detection during the enrichment phase, with a wide range of probes used in parallel
67 that hence allow a high selectivity. However, although antibodies or other protein probes have
68 been proven to have high efficiency as ligands (enabling strain or even serotype identification)
69 they are known to present several difficulties such poor stability, difficulty of production, high
70 cost, and/or burdensome handling. It is the reason why new sets of probes have been benched
71 by researchers, the most prominent being aptamers, molecularly imprinted polymers, and
72 peptides [12]. Aptamers and molecularly imprinted polymers usually show high specificity and
73 reliability [13,14]. Nevertheless, to achieve wide spectrum detection, the multiplexing of large
74 series of probing ligands remains an issue, which limits the extent of wide spectrum detection.

75 Antimicrobial peptides (AMPs) are a subset of peptides presenting outstanding bactericidal
 76 activity [15,16]. Their binding to bacteria mainly relies on physico-chemical interactions, due to
 77 their polycationic or amphiphilic characteristics. Hence, they can easily attach to negatively
 78 charged lipopolysaccharides (LPS) anchored in the membrane of Gram-negative bacteria *via*
 79 electrostatic interactions [17,18]. Conformational changes of their structure can also mediate the
 80 attachment to bacterial outer walls [19]. Although AMPs have so far mainly been investigated to
 81 design new drugs or antimicrobial applications [20], they are also promising ligands as potential
 82 alternatives to antibodies as large spectrum recognition elements towards bacteria [21,22].
 83 Indeed, they have naturally evolved to interact with a wide range of pathogenic bacteria and they
 84 are not only easy to synthesize but also easier to handle than antibodies for instance, since they
 85 can resist harsh chemical conditions and air-drying for storage.

86 Surprisingly, the use of AMPs as recognition elements has only rarely been commented on in
 87 the literature [23–26]. Those studies relied on the specific recognition of particular groups of
 88 bacteria, for instance targeting either a bacterial genus or a Gram class. Herein, we demonstrate
 89 the use of AMPs in a multiplexed fashion, with several different peptidic probes exposed to a
 90 contaminated sample. Thanks to the development of antimicrobial peptides arrays, we expand
 91 the spectrum of detectable bacterial strains in a single one-step assay. Wide-spectrum sensing
 92 of bacterial pathogens would hence be achieved. A set of AMPs inspired by previous works on
 93 biosensors (see *Table 1*), has been produced by solid-phase synthesis and arrayed on the gold
 94 surface of SPRI prisms. Such arrays were then assayed with a series of samples spiked with
 95 pathogenic bacteria at low levels. Those strains are representative of major species encountered
 96 in both foodborne infections and bacteremia. We were thus able to assess the performance of
 97 such peptide-based sensors for wide-spectrum detection of bacteria.

98 Material and methods

99 Reagents

100 Phosphate Buffered Saline (PBS), Dimethyl Sulfoxide (DMSO), Bovine Serum Albumin (BSA),
 101 glycerol and Tryptic Soy Broth (TSB) culture medium were purchased from Sigma-Aldrich (Saint
 102 Quentin Fallavier, France). The solid culture medium Tryptone Soy Agar (TSA) was bought from
 103 bioMérieux (Lyon, France). Ultra-pure water (18,2 *M.Ω* of resistivity) was obtained from an ELGA
 104 PURELAB flex dispenser (Veolia Water, France).

105 Peptides

106

Name	Sequence	Targets	Technique	Ref.
Clavanin A	VFQFLGKIIHHVGNFVHGFSHFV-spacer-C-NH ₂	<i>E. coli</i> , <i>S. aureus</i> & <i>S. Typhimurium</i>	Electrochemical impedance	[27]
Magainin 1	GIGKFLHSAGKFGKAFVGEIMKS-spacer-C-NH ₂	<i>E. coli</i> & <i>S.</i> <i>Typhimurium</i>	Fluorescence	[28]
		<i>E. coli</i> & <i>Salmonella</i>	Electrochemical capacitance	[24]
		<i>E. coli</i>	Fluorescence	[29]
		<i>E. coli</i>	Field-effect transistor	[30]
Pediocin Ped3	GKATTCIINNGAMA-spacer-C-NH ₂	<i>Listeria</i>	Microcantilevers	[31]

PGQ	GVLSNVIGYLKKGALNAVLKQ-spacer-C-NH ₂	<i>monocytogenes</i> <i>E. coli</i>	Fluorescence	[32]
Leucocin A 24	C-spacer-SVNWGEAFSAGVHRLANGNGFW-OH	<i>Listeria</i> <i>monocytogenes</i> & <i>E. coli</i>	Electrochemical impedance	[25, 33]
Control peptide	C-spacer-RGEWFWGNLVVSAASFGNHNAGG-OH	Scrambled version of Leucocin A 24 (newly introduced)		

107 *Table 1. Set of arrayed antimicrobial peptides. Sequences are listed along with the bacteria they*
 108 *can detect, the detection techniques that they were used in and literature references for each.*
 109 *Spacer is corresponding to AEEA.*

110

111 All peptides were synthesized by Smart Bioscience (Saint Égrève, France) through standard
 112 Fmoc solid-phase method. A (2-(2-(amino)ethoxy)ethoxy)acetic acid (AEEA) spacer was
 113 inserted between the peptide sequence and the additional terminal cysteine. When this cysteine
 114 amino acid was added at the C-terminus, the supplier amidated this latter to achieve higher
 115 synthesis yields, otherwise the terminal amino acid was left free. The sequences of the chosen
 116 peptides are listed in *Table 1*. The certificates of analysis furnished by Smart Bioscience are
 117 given in the Electronic Supplementary Information to confirm peptide purities and molecular
 118 weights.

119 Bacterial strains

120 The *Salmonella enterica* subspecies *enterica* serovar Typhimurium (*S. Typhimurium*),
 121 CIP104474, was obtained from the Pasteur Institute (Paris, France). *Listeria monocytogenes*
 122 strain belonging to the molecular serotype IVc was acquired from the Institut Scientifique
 123 d'Hygiène et d'Analyse (ISHA, Massy, France). It had been isolated from chicken meat. The
 124 methicillin-resistant *Staphylococcus aureus* subspecies *aureus* (MRSA), ATCC43300, the
 125 *Staphylococcus epidermidis* strain, ATCC12228, and the *Escherichia coli* serovar O1:K1:H7
 126 (isolated from urine), ATCC11775, were all purchased from the American Type Culture
 127 Collection (Manassas, Virginia, USA).

128 Culture conditions

129 Prior to each experiment, an individual bacterial colony was isolated on a TSA plate and
 130 resuspended in 4 mL of sterile TSB. This bacterial culture was then incubated for 18 hours at
 131 37°C under constant agitation (180 rpm). Ten-fold serial dilutions of the bacterial suspension
 132 were then performed in TSB. 100 μL of one of the ten-fold dilution series was used for sample
 133 spiking. The 10^{-5} and 10^{-6} dilutions were plated (100 μL on TSA plates, in triplicates) to
 134 determine the initial bacterial concentration through manual colony counting. For each assay,
 135 sterility controls were performed.

136 Peptide arraying

137 Lyophilized peptides were resuspended in DMSO at 1 $\text{mg}\cdot\text{mL}^{-1}$ and stored at -80°C. Each
 138 peptide sequence was diluted at 100 μM in PBS 1x, with 5% (v/v) of glycerol ahead of arraying
 139 biochips. SPRI-biochips bought from Horiba Scientific (Palaiseau, France) consisted of glass
 140 prisms coated with a thin gold layer for direct functionalization using thiol moieties (see fig. S1 in
 141 the Electronic Supplementary Information for more details). Peptide biochips were prepared

142 using a sciFLEXARRAYER (Scienion, Berlin, Germany), a piezo-dispenser allowing arraying of
143 4 *nL* droplets per spot. Each array resulted in 12 spots with a 450 μm diameter, and a 800 μm
144 pitch between each spot. All peptides were systematically arrayed in duplicate. This step was
145 performed at room temperature under a humid atmosphere (75% relative humidity). After
146 arraying, prisms were incubated for 18 hours at 25°C, under 94% humidity, to allow the
147 complete formation of self-assembled monolayers of peptides onto gold. Chips were then rinsed
148 with ultra-pure water, dried under an argon flow for a few seconds, and stored up to several
149 weeks at +4°C until experiments. Effective surface functionalization was assessed by AFM
150 comparison with bare gold surfaces (supplemental figure S2).

151 Biochip conditioning and sample processing

152 Prisms were systematically incubated with a sterile solution of PBS+1% BSA before each
153 experiment to mimic interfering proteins of complex media such as blood, and to block non-
154 specific interactions with gold. The surface of the prism was then rinsed with 3 mL of sterile PBS,
155 before loading the biochip in the Surface Plasmon Resonance imager. 900 μL of sterile TSB
156 were then injected in the culture chamber containing the AMP-array, followed by 100 μL of the
157 bacterial dilution used for spiking. Interactions of bacteria on the surface of the prisms were
158 observed in real-time with the SPRi-Lab+ system (Horiba Scientific, Palaiseau, France), at 37°C.
159 The AMP-array was positioned so that its surface was vertical, on the sidewall of the culture
160 chamber. This avoids any non-specific signal from sedimenting bacteria. Sensors were
161 systematically discarded after use.

162 SPR data analysis

163 Real-time monitoring of the SPR signal began when the bacteria were spiked into the sample.
164 Regions of interest (ROI) were defined on each duplicate of AMP spots, in order to monitor the
165 temporal change of reflectivity. Kinetics data were directly collected and processed in R
166 programming language. Duplicate spots of each peptide were averaged, corrected with respect
167 to the reference signal, and plotted. Peptide-free gold ROIs, coated with BSA, were chosen as
168 reference signals for non-specific interactions. Reflectivity shifts as a function of time for each
169 ROI allowed the assessment of the presence of bacteria in samples without further processing of
170 the data, by the observation of a temporal response shift. Kinetics data were used to generate a
171 database of interaction patterns between peptides and bacteria. For each spot, the first
172 derivative of the smoothed temporal data was calculated. The maximum value of this derivative,
173 as well as the corresponding smoothed reflectivity shift, were recorded. Unsupervised
174 multivariate analysis was performed on this database thanks to the FactomineR package,
175 embedded in the R software [34]. Names of targeted bacteria were used as a descriptive
176 variable, and therefore did not affect the results of the Principal Components Analysis (PCA). As
177 data were heterogeneous, they were centered and reduced. On one hand, PCA score plots were
178 used to distinguish results from one bacterial strain to another. On the other hand, they also
179 permitted a high level of repeatability of the process from different duplicates of the same assay.
180 Hierarchical Clustering on Principal Components (HCPC) was also performed on the outcome of
181 the PCA. This statistical method ensured that targeted bacteria were indeed discriminated from
182 each other, based on the Euclidean distance separating the replicates in the PCA results.

183

184

Results and discussion

185

Bacterial growth monitoring by SPRI

186

The set of five bacterial strains to be detected with the peptide array has been chosen to represent the diversity of pathogens frequently involved in bloodstream or urinary tract infections, as well as food poisoning. The set also reflects microbial morphological diversity, with both Gram-positive and negative species, including bacilli and cocci.

187

Growth kinetics monitored by SPRI of the bacteria are depicted in fig. 1, datasets retrieved from those results allow defining characteristic detection times of bacteria (Supplemental Table S1) and affinity patterns with the peptides.

188

189

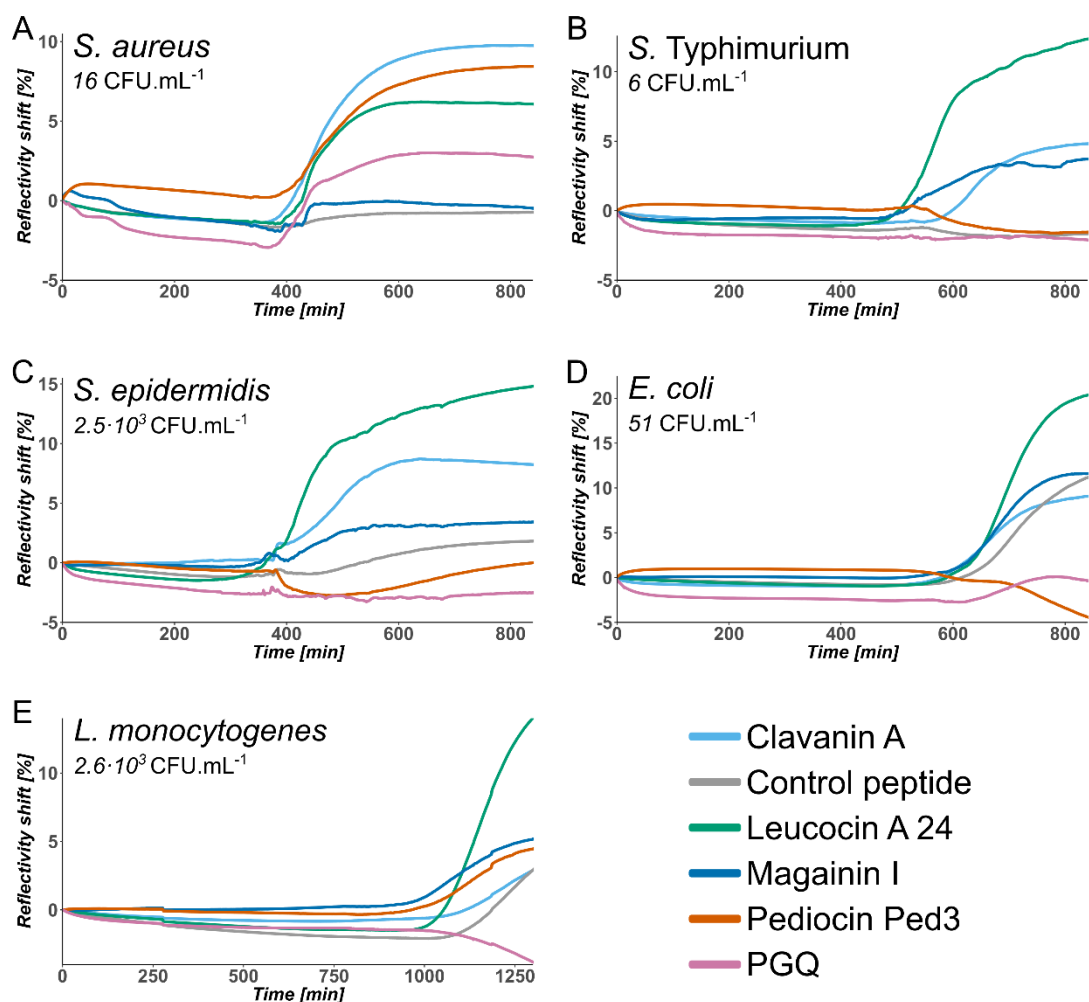
190

Growth kinetics monitored by SPRI of the bacteria are depicted in fig. 1, datasets retrieved from those results allow defining characteristic detection times of bacteria (Supplemental Table S1) and affinity patterns with the peptides.

191

192

193



194

195

Figure 1. SPR kinetic data of the bacterial growth for five different bacterial strains cultured in tryptic soy broth at 37°C. Each curve is the average of duplicate spots for a given peptide arrayed on the sensor, with subtraction of the reference signal taken on peptide free gold.

196

197

198 AMP-based arrays have permitted the detection of pathogens present at low initial concentration
199 in all samples, at most in 19 hours, and in even less than 12 hours in the majority of cases. All
200 culture conditions being the same, variations of detection signal can come from dissimilarities in
201 generation times of the different strains. Shortest detection times were for *S. aureus* and *S.*
202 *epidermidis*, in about 6 to 7 hours. Similar conclusions with solid based culture methods are
203 hitherto obtained in at least 24 hours. Compared to other biosensing methods using AMPs to
204 analyze pre-enriched samples, we obtained a very low limit of detection of virtually one live
205 bacterium per sample. The coupling of the enrichment step in our one-step process, not only
206 improved the safety for the operator, but also significantly improved both the overall processing
207 time and the limit of detection, by comparison to the two-steps methods described so far.
208 Naturally, the lower limit of detection comes with a longer detection time to get bacterial
209 concentrations sufficient for SPRI detection.

210 Individual peptide responses for bacterial pathogens detection

211 Peptides showed very distinct profiles of response depending on the targeted bacterial strains.
212 Individual examination of their performances is thus interesting to understand underlying
213 interactions with bacteria. Interestingly, Leucocin A 24 interacted strongly with all tested bacterial
214 strains. Nonetheless, the scrambled version of Leucocin A 24, here used as a control peptide,
215 displayed only weak to no interactions at all with any bacterial pathogen, suggesting that
216 interactions of bacteria with tethered peptides are not only governed by physico-chemical
217 mechanisms but more probably by structural interactions between peptides and bacterial
218 membranes. Such observation has already been described for therapeutic peptides [35].
219 Clavanin A functionalized surfaces exhibited stronger SPRI responses with *Staphylococci spp.*,
220 which are Gram-positive bacteria, although this peptide also enabled to successfully detect
221 *Salmonella Typhimurium* and *E. coli*, although with weaker interactions. With our method,
222 Magainin I only displayed mild interactions with all the tested bacteria, whatever their Gram
223 coloration (except for *S. aureus* which gave a very low shift). On the contrary, Ped3, a Pediocin
224 fragment, exhibited a moderate ability to detect *Listeria monocytogenes*, as previously described
225 [31], but surprisingly Ped3 also displayed a potent interaction with MRSA in our assay. In the
226 meantime it did not interact with *S. epidermidis*, although they belong to the same *genus*. This
227 selective response might be caused by an association of the peptide with a peculiar receptor
228 specific to the membrane of MRSA. PGQ displayed interactions with *E. coli*, which is consistent
229 with the literature [32]. However it detected *S. aureus*, which is a Gram-positive strain, and had
230 no apparent interactions with *Salmonella*, another Gram-negative bacterium, that also displays
231 LPS, which is a hint that the interactions between PGQ and bacteria is not only mediated by
232 interacting with the latter.

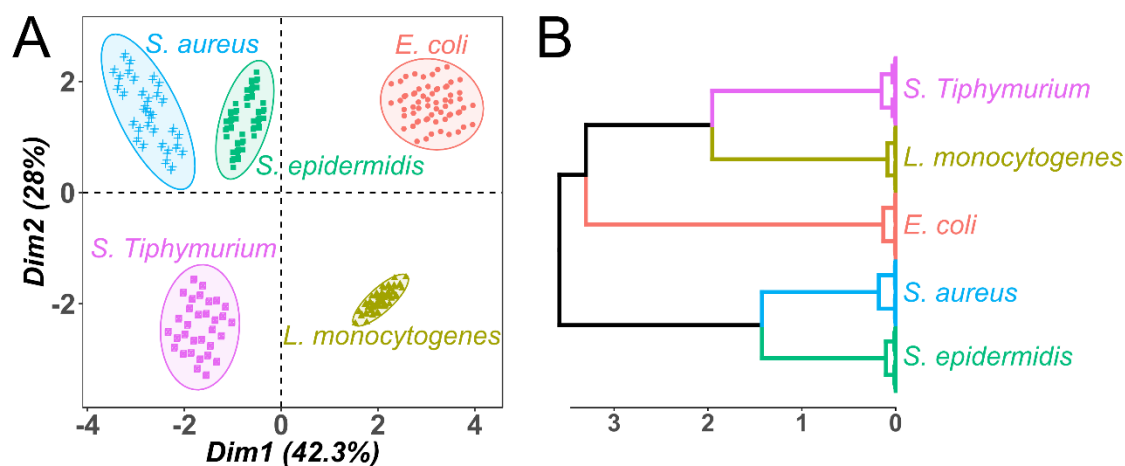
233 These results tend to show that AMPs keep a wide spectrum of affinity towards bacteria after
234 tethering on a surface. Moreover, association of AMPs enabled to obtain various kinetic profiles
235 depending on the bacterial strain. Interestingly, our SPRI detection method allowed to unravel
236 interactions which remained unobserved with other methods [25]. This could be explained by the
237 establishment of weaker interactions between bacteria and AMPs thanks to their longer
238 exposure time to the cultured bacteria.

239 Multivariate analyses of kinetic results

240 Multivariate analyses were performed to objectively assess the discrimination values of our
241 method. To do so, PCA was performed based on reflectivity shift and sensitivity values at the

242 maximum of the first derivative for each peptide (Figure 2A). Each bacterial strain was
 243 processed once on an AMP micro-array, giving 64 sets of values, from all possible combinations
 244 of peptide duplicates responses at the surface. This combinatorial analyzing method ensured
 245 that statistical variability of the overall response was totally represented, and that cherry picking
 246 of data was avoided. Experiments on different bacterial strains with the same set of AMPs gave
 247 clustered results in the PCA 2D-score plot. Moreover, those clusters of data points were well
 248 segregated from each other according to the monitored pathogen: results were repeatable
 249 regardless of the set of replicates in the same monitoring. The first two principal components
 250 represented only 70.3% of the total variance. This meant that the data were of high
 251 dimensionality, thus explaining why such a good discrimination between bacterial strains could
 252 be obtained. However, those first two components were sufficient in our case to clearly
 253 distinguish between distinct bacterial strains. Such results underlined potential identification
 254 ability of the method, although more experiments would be required to create an even more
 255 exhaustive database. Results of the PCA were also used to perform a Hierarchical Clustering on
 256 Principal Components (fig. 2B), leading again to a satisfying separation of the different strains in
 257 separate clusters. Such discriminated profiles came from the variety of affinities displayed by the
 258 peptides towards the tested bacteria. Due to different physicochemical properties and structures,
 259 each peptide interacted differently to Gram or genera, hence the overall combination
 260 discriminated the tested strains. Multivariate analyses with appropriate databases thus allow
 261 pathogen identification methods to be derived from the usual key-lock principle and enable
 262 cross-reactivity sensors as demonstrated by [36].

263



264

265 *Figure 2. Multivariate data analyses for 5 bacterial strains processed on AMP-arrays. (A) 2D-*
 266 *score plot of the database generated from the kinetics of SPRI bacterial growth monitoring.*
 267 *Ellipses were annotated to represent the 95% confidence interval. (B) Hierarchical Clustering on*
 268 *Principal Components (HCPC) performed on the data from Fig. 2a. Distances between points*
 269 *are Euclidean.*

270

271 In this work, we demonstrated the suitability of AMP-arrays as powerful ligands of bacterial
 272 pathogens. Traditionally studied in the field of pharmacology and antimicrobial applications,
 273 AMPs were revealed to be potent ligands for pathogens in biosensing applications. Not only they
 274 are well-adapted for the detection of bacteria in a standard culture medium such as tryptic soy

275 broth, but compared to antibodies, the biochip functionalization and operation were less tedious,
276 thanks to peptide resistance to air-drying without loss of activity in the process.

277 The use of AMPs in a multiplexed fashion allowed a fast and simple assessment of the presence
278 of pathogens even at low concentrations. Detection times ranged from 6 to 19 hours, in a one-
279 step assay. This is shorter than standard methods in blood or foodstuffs, which require
280 enrichment times of usually 24 hours before confirmation of the culture positivity. Each tested
281 bacterial strain resulted in different kinetic responses on the part of the AMP-array. Ped3 even
282 exhibited a near-specific behavior, interacting almost uniquely with MRSA. Further studies could
283 assess this point, which would be of importance in the detection of this prominent pathogen. Our
284 results, for instance for Leucocin A24 and its scrambled version, showed that the recognition of
285 bacteria by AMPs is not uniquely driven by physico-chemical interactions, but also by their
286 secondary structuration. Moreover, tethering of the AMPs on the surface of our sensor did not
287 seem to alter this interaction with bacteria in solution. The study of the whole set of AMPs
288 interacting with live bacteria gave clearly different affinity profiles. This combined approach was
289 preferred to a biomolecular study to enable the identification of several bacterial pathogens, with
290 a single AMP set. The response to polymicrobial infections, which represent only 10% of
291 bloodstream infections [37,38], is still to be investigated to check how AMPs responses might be
292 deciphered to identify two, or more, pathogenic strains present in the same sample.

293 Furthermore, the small set of AMPs we used provided very distinct affinity profiles towards
294 different pathogens, as multivariate analysis confirmed. Arrays presenting a larger collection of
295 peptides could hence enable the possibility to create interaction profile libraries and therefore the
296 identification of bacterial genus, species or strain of the infecting pathogen in a sample.

297 To the extent of our knowledge, the system we described is the first one-step biosensor assay
298 using different multiplexed AMPs and enabling detection of several viable bacterial strains in
299 biomedically relevant concentrations along with a discrimination capacity in a label-free assay. In
300 the near future, this approach could be applied for the detection of any pathogen in samples
301 such as foodstuff, urine or blood without any pre-requisite knowledge of the threat.

302 If these auspicious results are confirmed on a larger scale, it could permit the development of a
303 one-step assay – not only able to detect common pathogens overnight – but also to identify
304 them in reference to a database of affinity patterns.

305

306

Color should be used for any figures in print

307

308

309 Acknowledgements

310 EP thanks the Labex ARCANE and CBH-EUR-GS program (ANR-17-EURE-0003) for his
311 doctoral fellowship.

312

313 Competing interests statement

314 The authors declare no financial or non-financial competing interests.

315

316 References

- 317 [1] A. van Belkum, G. Durand, M. Peyret, S. Chatellier, G. Zambardi, J. Schrenzel, D. Shortridge,
318 A. Engelhardt, W.M. Dunne, Rapid clinical bacteriology and its future impact, *Ann. Lab. Med.* 33
319 (2013) 14, <https://doi.org/10.3343/alm.2013.33.1.14>.
- 320 [2] O. Opota, K. Jaton, G. Greub, Microbial diagnosis of bloodstream infection: Towards
321 molecular diagnosis directly from blood, *Clin. Microbiol. Infec.* 21 (2015) 323–331,
322 <https://doi.org/10.1016/j.cmi.2015.02.005>.
- 323 [3] A.E. Clark, E.J. Kaleta, A. Arora, D.M. Wolk, Matrix-assisted laser desorption ionization-time
324 of flight mass spectrometry: A fundamental shift in the routine practice of clinical microbiology,
325 *Clin. Microbiol. Rev.* 26 (2013) 547–603, <https://doi.org/10.1128/cmr.00072-12>.
- 326 [4] M. Guido Marcello, M.R. Tumolo, A. De Donno, T. Verri, F. Serio, F. Bagordo, A. Zizza, In
327 vitro diagnosis of sepsis: A review, *Pathol. Lab. Med. Int.* (2016) 1,
328 <https://doi.org/10.2147/plmi.s49800>.
- 329 [5] D.C. Vanegas, C.L. Gomes, N.D. Cavallaro, D. Giraldo-Escobar, E.S. McLamore, Emerging
330 biorecognition and transduction schemes for rapid detection of pathogenic bacteria in food,
331 *Compr. Rev. Food Sci. F.* (2017), <https://doi.org/10.1111/1541-4337.12294>.
- 332 [6] E. Suraniti, E. Sollier, R. Calemczuk, T. Livache, P.N. Marche, M.-B. Villiers, Y. Roupioz,
333 Real-time detection of lymphocytes binding on an antibody chip using SPR imaging, *Lab Chip.* 7
334 (2007) 1206, <https://doi.org/10.1039/b708292d>.
- 335 [7] J.B. Fiche, J. Fuchs, A. Buhot, R. Calemczuk, T. Livache, Point mutation detection by surface
336 plasmon resonance imaging coupled with a temperature scan method in a model system, *Anal.*
337 *Chem.* 80 (2008) 1049–1057, <https://doi.org/10.1021/ac7019877>.
- 338 [8] S. Bouguelia, Y. Roupioz, S. Slimani, L. Mondani, M.G. Casabona, C. Durmort, T. Vernet, R.
339 Calemczuk, T. Livache, On-chip microbial culture for the specific detection of very low levels of
340 bacteria, *Lab Chip.* 13 (2013) 4024, <https://doi.org/10.1039/c3lc50473e>.
- 341 [9] L. Mondani, Y. Roupioz, S. Delannoy, P. Fach, T. Livache, Simultaneous enrichment and
342 optical detection of low levels of stressed *Escherichia coli* O157:H7 in food matrices, *J. Appl.*
343 *Microbiol.* 117 (2014) 537–546, <https://doi.org/10.1111/jam.12522>.
- 344 [10] A. Morlay, A. Duquenoy, F. Piat, R. Calemczuk, T. Mercey, T. Livache, Y. Roupioz, Label-
345 free immuno-sensors for the fast detection of listeria in food, *Measurement.* 98 (2017) 305–310,
346 <https://doi.org/10.1016/j.measurement.2016.06.038>.

- 347 [11] V. Templier, T. Livache, S. Boisset, M. Maurin, S. Slimani, R. Mathey, Y. Roupioz, Biochips
348 for direct detection and identification of bacteria in blood culture-like conditions, Sci. Rep. 7
349 (2017), <https://doi.org/10.1038/s41598-017-10072-z>.
- 350 [12] V. Templier, A. Roux, Y. Roupioz, T. Livache, Ligands for label-free detection of whole
351 bacteria on biosensors: A review, TrAC Trend. Anal. Chem. 79 (2016) 71–79,
352 <https://doi.org/10.1016/j.trac.2015.10.015>.
- 353 [13] R. Singh, M.D. Mukherjee, G. Sumana, R.K. Gupta, S. Sood, B. Malhotra, Biosensors for
354 pathogen detection: A smart approach towards clinical diagnosis, Sensor. Actuat. B-Chem. 197
355 (2014) 385–404, <https://doi.org/10.1016/j.snb.2014.03.005>.
- 356 [14] M. Shahdordizadeh, S.M. Taghdisi, N. Ansari, F.A. Langroodi, K. Abnous, M. Ramezani,
357 Aptamer based biosensors for detection of *Staphylococcus aureus*, Sensor. Actuat. B-Chem.
358 241 (2017) 619–635, <https://doi.org/10.1016/j.snb.2016.10.088>.
- 359 [15] M. Zasloff, Antimicrobial peptides of multicellular organisms, Nature. 415 (2002) 389–395,
360 <https://doi.org/10.1038/415389a>.
- 361 [16] H.G. Boman, Antibacterial peptides: Basic facts and emerging concepts, J. Intern. Med. 254
362 (2003) 197–215, <https://doi.org/10.1046/j.1365-2796.2003.01228.x>.
- 363 [17] M.R. Yeaman, Mechanisms of antimicrobial peptide action and resistance, Pharmacol. Rev.
364 55 (2003) 27–55, <https://doi.org/10.1124/pr.55.1.2>.
- 365 [18] L.T. Nguyen, E.F. Haney, H.J. Vogel, The expanding scope of antimicrobial peptide
366 structures and their modes of action, Trends Biotechnol. 29 (2011) 464–472,
367 <https://doi.org/10.1016/j.tibtech.2011.05.001>.
- 368 [19] M. Torrent, J. Valle, M.V. Nogués, E. Boix, D. Andreu, The generation of antimicrobial
369 peptide activity: A trade-off between charge and aggregation?, Angew. Chem. Int. Edit. 50
370 (2011) 10686–10689, <https://doi.org/10.1002/anie.201103589>.
- 371 [20] A.K. Marr, W.J. Gooderham, R.E. Hancock, Antibacterial peptides for therapeutic use:
372 Obstacles and realistic outlook, Curr. Opin. Pharmacol. 6 (2006) 468–472,
373 <https://doi.org/10.1016/j.coph.2006.04.006>.
- 374 [21] R.R. Silva, K.Y.P.S. Avelino, K.L. Ribeiro, O.L. Franco, M.D.L. Oliveira, C.A.S. Andrade,
375 Optical and dielectric sensors based on antimicrobial peptides for microorganism diagnosis,
376 Front. Microbiol. 5 (2014), <https://doi.org/10.3389/fmicb.2014.00443>.
- 377 [22] M. Hoyos-Nogués, F.J. Gil, C. Mas-Moruno, Antimicrobial peptides: Powerful biorecognition
378 elements to detect bacteria in biosensing technologies, Molecules. 23 (2018) 1683,
379 <https://doi.org/10.3390/molecules23071683>.
- 380 [23] N. Kulagina, K. Shaffer, F. Ligler, C. Taitt, Antimicrobial peptides as new recognition
381 molecules for screening challenging species, Sensor. Actuat. B-Chem. 121 (2007) 150–157,
382 <https://doi.org/10.1016/j.snb.2006.09.044>.
- 383 [24] M.S. Mannoor, S. Zhang, A.J. Link, M.C. McAlpine, Electrical detection of pathogenic
384 bacteria via immobilized antimicrobial peptides, P. Natl. Acad. Sci USA. 107 (2010) 19207–
385 19212, <https://doi.org/10.1073/pnas.1008768107>.

- 386 [25] H. Etayash, L. Norman, T. Thundat, K. Kaur, Peptide-bacteria interactions using engineered
387 surface-immobilized peptides from class IIa bacteriocins, *Langmuir*. 29 (2013) 4048–4056,
388 <https://doi.org/10.1021/la3041743>.
- 389 [26] C.A. Andrade, J.M. Nascimento, I.S. Oliveira, C.V. de Oliveira, C.P. de Melo, O.L. Franco,
390 M.D. Oliveira, Nanostructured sensor based on carbon nanotubes and clavanin A for bacterial
391 detection, *Colloid. Surface. B*. 135 (2015) 833–839,
392 <https://doi.org/10.1016/j.colsurfb.2015.03.037>.
- 393 [27] A.G.S. Junior, M.D. Oliveira, I.S. Oliveira, R.G. Lima-Neto, S.R. Sá, O.L. Franco, C.A.
394 Andrade, A simple nanostructured impedimetric biosensor based on clavanin A peptide for
395 bacterial detection, *Sensor. Actuat. B-Chem*. 255 (2018) 3267–3274,
396 <https://doi.org/10.1016/j.snb.2017.09.153>.
- 397 [28] N.V. Kulagina, M.E. Lassman, F.S. Ligler, C.R. Taitt, Antimicrobial peptides for detection of
398 bacteria in biosensor assays, *Anal. Chem*. 77 (2005) 6504–6508,
399 <https://doi.org/10.1021/ac050639r>.
- 400 [29] M.-S. Chang, J.H. Yoo, D.H. Woo, M.-S. Chun, Efficient detection of *Escherichia coli*
401 O157:H7 using a reusable microfluidic chip embedded with antimicrobial peptide-labeled beads,
402 *Analyst*. 140 (2015) 7997–8006, <https://doi.org/10.1039/c5an01307k>.
- 403 [30] Y. Chen, Z.P. Michael, G.P. Kotchey, Y. Zhao, A. Star, Electronic detection of bacteria using
404 holey reduced graphene oxide, *ACS Appl. Mater. Inter*. 6 (2014) 3805–3810,
405 <https://doi.org/10.1021/am500364f>.
- 406 [31] S. Azmi, K. Jiang, M. Stiles, T. Thundat, K. Kaur, Detection of *Listeria monocytogenes* with
407 short peptide fragments from class IIa bacteriocins as recognition elements, *ACS Comb. Sci*. 17
408 (2015) 156–163, <https://doi.org/10.1021/co500079k>.
- 409 [32] S. Arcidiacono, P. Pivarnik, C.M. Mello, A. Senecal, Cy5 labeled antimicrobial peptides for
410 enhanced detection of *Escherichia coli* O157:H7, *Biosens. Bioelectron*. 23 (2008) 1721–1727,
411 <https://doi.org/10.1016/j.bios.2008.02.005>.
- 412 [33] H. Etayash, L. Norman, T. Thundat, M. Stiles, K. Kaur, Surface-conjugated antimicrobial
413 peptide leucocin A displays high binding to pathogenic Gram-positive bacteria, *ACS Appl. Mater.*
414 *Inter*. 6 (2014) 1131–1138, <https://doi.org/10.1021/am404729c>.
- 415 [34] S. Lê, J. Josse, F. Husson, FactoMineR: An R package for multivariate analysis, *J. Stat.*
416 *Softw*. 25 (2008), <https://doi.org/10.18637/jss.v025.i01>.
- 417 [35] C.D. Fjell, J.A. Hiss, R.E.W. Hancock, G. Schneider, Designing antimicrobial peptides: Form
418 follows function, *Nat. Rev. Drug Discov*. (2011), <https://doi.org/10.1038/nrd3591>.
- 419 [36] J.R. Carey, K.S. Suslick, K.I. Hulkower, J.A. Imlay, K.R.C. Imlay, C.K. Ingison, J.B. Ponder,
420 A. Sen, A.E. Wittrig, Rapid identification of bacteria with a disposable colorimetric sensing array,
421 *J. Am. Chem. Soc*. 133 (2011) 7571–7576, <https://doi.org/10.1021/ja201634d>.
- 422 [37] M. Pavlaki, G. Poulakou, P. Drimousis, G. Adamis, E. Apostolidou, N.K. Gatselis, I. Kritselis,
423 A. Mega, V. Mylona, A. Papatsoris, A. Pappas, A. Prekates, M. Raftogiannis, K. Rigaki, K.
424 Sereti, D. Sinapidis, I. Tsangaris, V. Tzanetakou, D. Veldekis, K. Mandragos, H. Giamarellou, G.

425 Dimopoulos, Polymicrobial bloodstream infections: Epidemiology and impact on mortality, J Glob
426 Antimicrob Re. 1 (2013) 207-212, <https://doi.org/10.1016/j.jgar.2013.06.005>.

427 [38] C. Royo-Cebrecos, C. Gudiol, C. Ardanuy, H. Pomares, M. Calvo, J. Carratalà, A fresh look
428 at polymicrobial bloodstream infection in cancer patients, PLoS One, 12 (2017),
429 <https://doi.org/10.1371/journal.pone.0185768>.

Supplementary Information:

Antimicrobial peptide arrays for wide spectrum sensing of pathogenic bacteria

Éric Pardoux^{a,b}, Agnès Roux^a, Raphaël Mathey^a, Didier Boturyn^b, Yoann Roupioz^{a,*}

^aUniv. Grenoble Alpes, CNRS, CEA, INAC-SyMMES, 38000 Grenoble, France

^bUniv. Grenoble Alpes, CNRS, DCM, 38000 Grenoble, France

*Corresponding author: yoann.roupioz@cea.fr

Table S1. Detection times of the presence of the different bacterial strains are determined by the timestamp of the kinetics first derivative highest value. It thus corresponds to the middle of the jump between the baseline signal and the plateau. It is given for the shortest time for each bacterial strain, associated with the peptide giving this result. Only peptides giving a strong positive signal are included in the analysis. Times are given as the average over duplicates of each peptide.

Bacterial strain	Initial concentration (CFU.mL⁻¹)	Shortest detection time (min)	Peptide
<i>E. coli</i> ATCC11775	51	677	Clavanin A
<i>S. Typhimurium</i> CIP104474	6	537	Magainin I
<i>S. aureus</i> ATCC43300	16	433	Leucocin A 24
<i>S. epidermidis</i> ATCC12228	2.5 · 10 ³	374	Leucocin A 24
<i>L. monocytogenes</i> IVc	2.6 · 10 ³	1160	Leucocin A 24

Figure S1. (A) Scaled scheme showing characteristic dimensions of the SPRi-biochip, including a representation of the observable field of view with the SPRi-Lab+. (B) Picture of a SPRi-biochip right after a spotting.

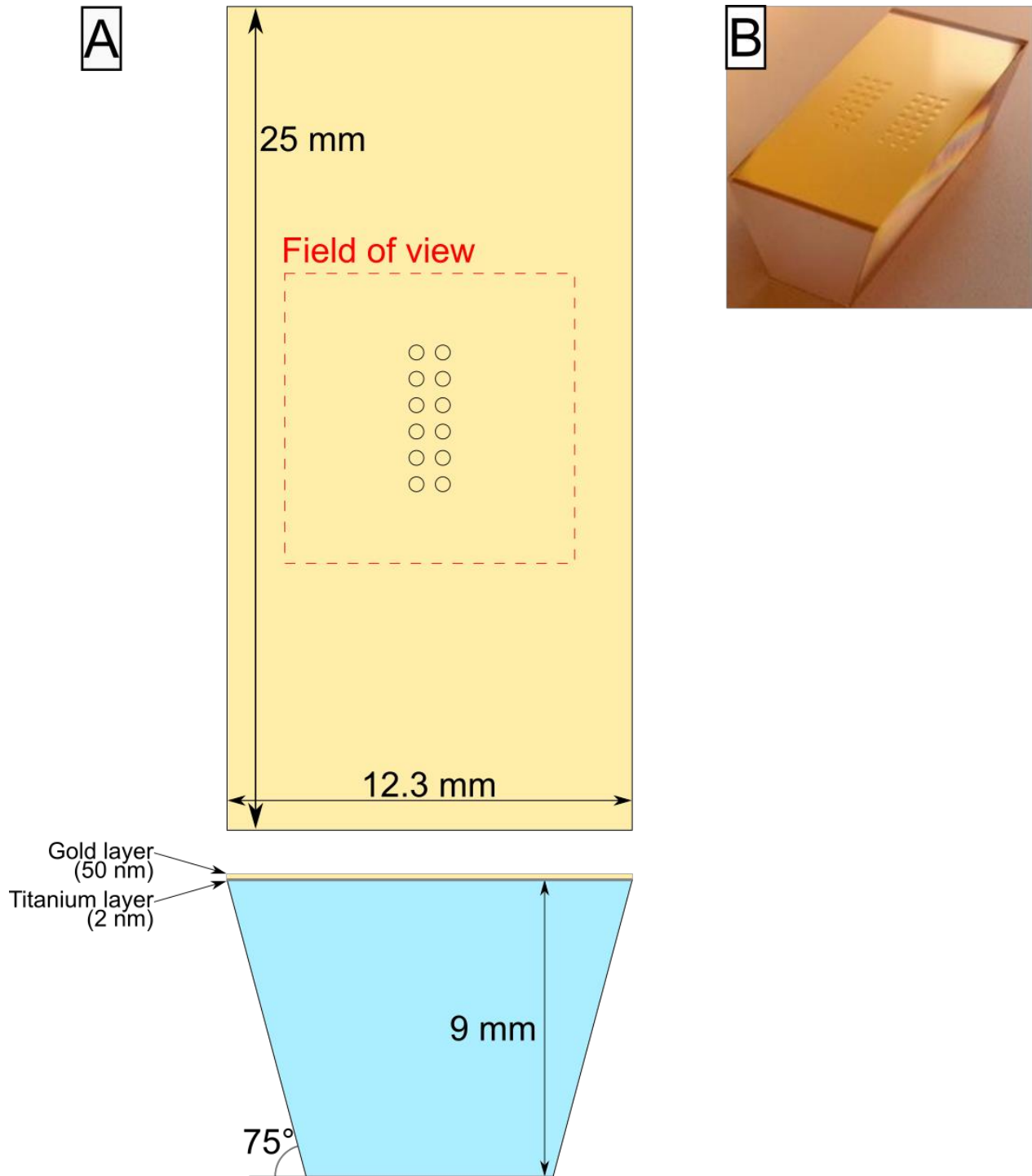
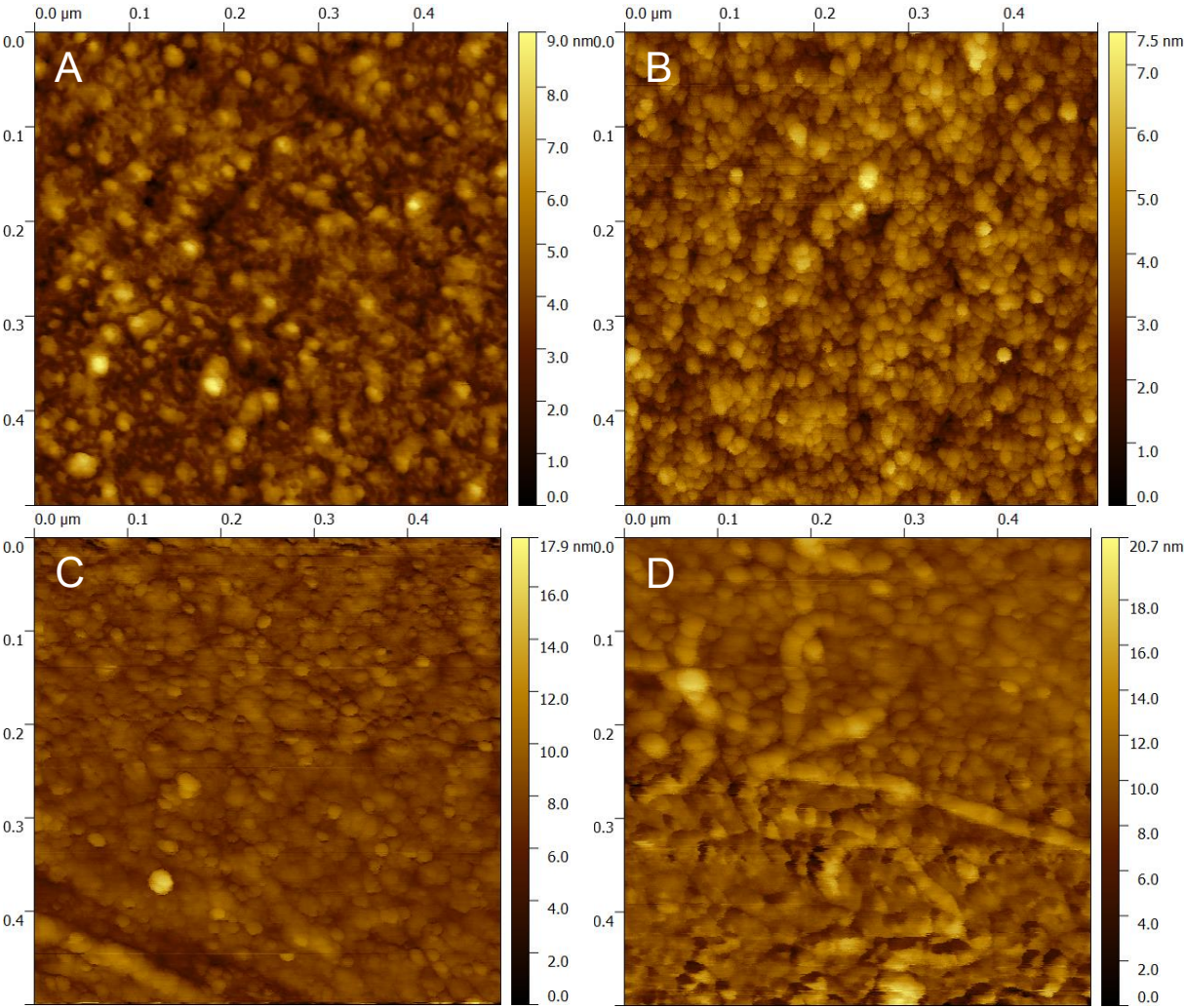


Figure S2. AFM images of monolayers of peptides prepared in the same conditions as SPRI biochips: (A) bare gold as a reference; (B) Magainin I; (C) Leucocin A 24; (D) Control peptide. They were recorded in air using the peak force mode of a Dimension Icon AFM (from Bruker, Santa Barbara, CA). The cantilevers were triangular and using a force contact of 0.1 N/m at a 70 kHz frequency and a 0.5 Hz scan rate. Image processing was performed using the Gwyddion microscopy software.



Certificate of analysis



Date	14/03/2016	Batch	849_s1p4f2
Product name	Magainin 1-Ncys	Catalog #	

Product specifications

AA sequence	C-AEEA-GIGKFLHSAGKFGKAFVGEIMKS-OH		
Disulfide bond	0		
Formula	$C_{121}H_{193}N_{31}O_{32}S_2$		
Appearance	White powder		
Theoretical average weight	2658,14 g/mol		
CAS number			
Source	Synthetic		
Counterion	TFA		
Solubility (recommendation)	10% acetonrile solution		1 mg/mL

Handling & Storage

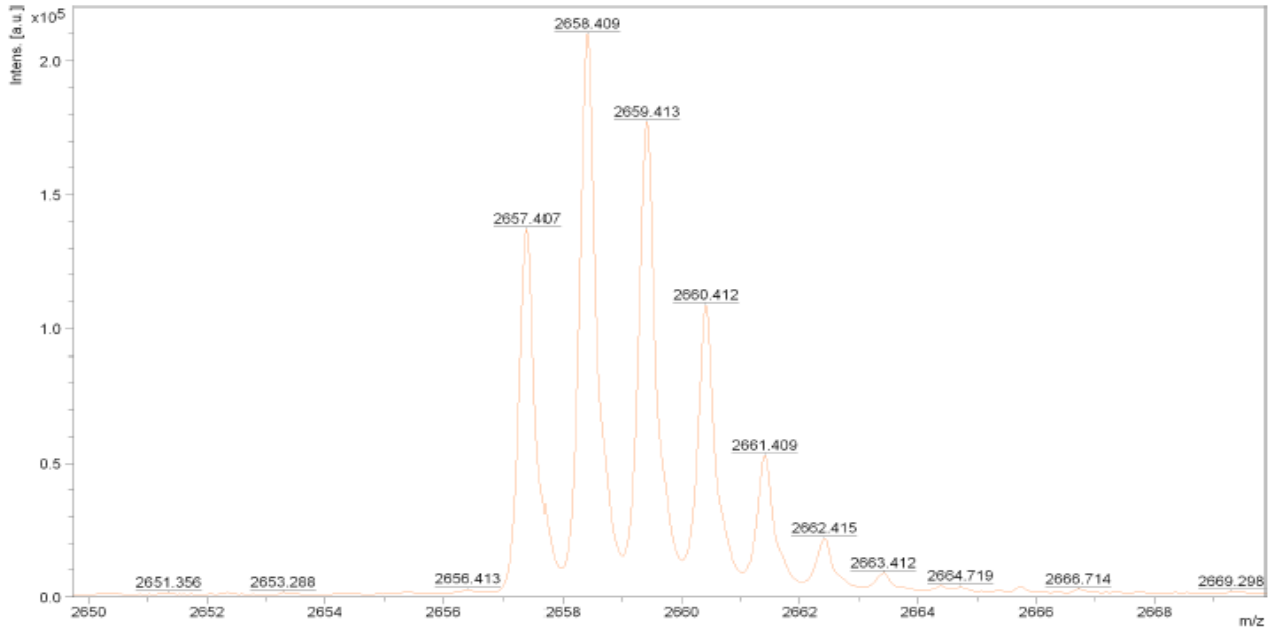
Storage	Shipped at ambient temperature under lyophilized powder. Store at -20°C (-4°F). Do not freeze-thaw. Aliquot sample if required and store at -80°C (-112°F).		
Expiry date	Not defined		
Handling and use restriction	Use with caution. Might be toxic. Product intended for research use only, not for use in diagnostic or therapeutic procedures.		

Analytical results

Observed purity rate	97,60%	Observed monoisotopic mass [M+H] ⁺	2657,407 Da
		Theoretical monoisotopic mass	2656,38 Da

Peak #	Time [min]	Area [$\mu\text{V}\cdot\text{s}$]	Height [μV]	Area [%]	Norm. Area [%]	BL	Area/Height [s]
-	0.001	0.00	0.00	0.00	0.00		-----
1	0.002	33.34	325.09	0.00	0.00	BV	0.1025
2	0.005	39.66	338.72	0.00	0.00	VV	0.1171
3	0.007	18.23	286.91	0.00	0.00	VV	0.0636
4	0.010	29.97	341.26	0.00	0.00	VB	0.0878
5	0.012	24.20	256.27	0.00	0.00	BV	0.0944
6	0.015	19.32	190.70	0.00	0.00	VB	0.1013
7	0.017	8.71	188.02	7e-05	7e-05	BV	0.0463
8	0.018	11.78	221.95	0.00	0.00	VB	0.0531
9	7.444	13.25	278.45	0.00	0.00	BV	0.0476
10	7.447	67.80	709.43	0.00	0.00	VV	0.0956
11	7.450	161.57	1440.70	0.00	0.00	VV	0.1121
12	7.530	11494288.40	2.54e+06	97.60	97.60	VE	4.5342
13	7.645	80123.98	70666.35	0.68	0.68	EV	1.1338
14	7.647	9323.03	72519.37	0.08	0.08	VV	0.1286
15	7.650	11590.99	72555.12	0.10	0.10	VV	0.1598
16	7.653	12378.38	72682.91	0.11	0.11	VV	0.1703
17	7.655	11828.25	72501.87	0.10	0.10	VV	0.1631
18	7.657	156665.19	72211.00	1.33	1.33	VE	2.1695
19	7.749	482.05	363.95	0.00	0.00	*EB	1.3245
		11777108.11	2.97e+06	100.00	100.00		

MS Spectra



D:\Data\Cermav\2016\Smartox\mars\160310\160310_magaininNoys_849_s1p4f2_rp\0_B71

printed: 3/14/2016 12:34:19 PM



+33 (0) 456 520 869



+33 (0) 456 520 868



contact@smartox-biotech.com

Smartox Biotechnology
570 rue de la chimie
38400 St Martin d'Hères
France

Certificate of analysis



Date	21/03/2016	Batch	847_s1p1f1
Product name	clavaninA	Catalog #	

Product specifications

AA sequence	VFQFLGKIIHHVGNFVHGFSHFV-AEEA-C-NH ₂		
Disulfide bond	0		
Formula	C ₁₄₀ H ₂₀₁ N ₃₇ O ₃₀ S		
Appearance	White powder		
Theoretical average weight	2914,39	g/mol	
CAS number			
Source	Synthetic		
Counterion	TFA		
Solubility (recommendation)	50% of Acetonitrile solution		1 mg/mL

Handling & Storage

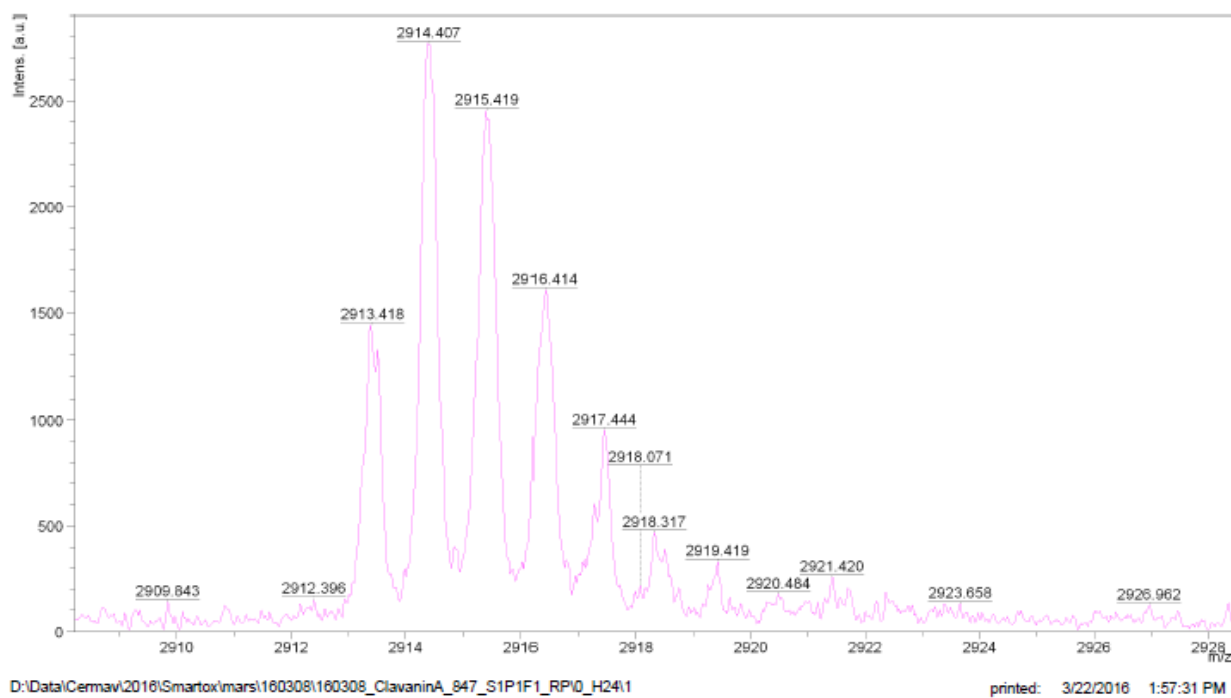
Storage	Shipped at ambient temperature under lyophilized powder. Store at -20°C (-4°F). Do not freeze-thaw. Aliquot sample if required and store at -80°C (-112°F).		
Expiry date	Not defined		
Handling and use restriction	Use with caution. Might be toxic. Product intended for research use only, not for use in diagnostic or therapeutic procedures.		

Analytical results

Observed purity rate	93,47%	Observed monoisotopic mass [M+H] ⁺	2913,41 Da
		Theoretical monoisotopic mass	2912,50 Da

Peak #	Time [min]	Area [$\mu\text{V}\cdot\text{s}$]	Height [μV]	Area [%]	Norm. Area [%]	BL	Area/Height [s]	Peak #	Time [min]	Area [$\mu\text{V}\cdot\text{s}$]	Height [μV]	Area [%]	Norm. Area [%]	BL	Area/Height [s]
-	0.001	0.00	0.00	0.00	0.00		-----	49	8.863	9991.57	69834.22	0.12	0.12	VV	0.1431
1	8.477	16.06	278.50	0.00	0.00	BB	0.0577	50	8.866	11781.87	70390.71	0.14	0.14	VV	0.1674
2	8.479	31.83	387.81	0.00	0.00	BB	0.0821	51	8.869	9892.04	70958.47	0.12	0.12	VV	0.1394
3	8.482	35.38	401.57	0.00	0.00	BV	0.0881	52	8.871	11412.92	71800.34	0.14	0.14	VV	0.1590
4	8.485	44.93	382.61	0.00	0.00	VV	0.1174	53	8.874	11541.86	72583.86	0.14	0.14	VV	0.1590
5	8.487	33.96	351.45	0.00	0.00	VB	0.0966	54	8.877	12634.93	73338.95	0.15	0.15	VV	0.1723
6	8.490	42.92	404.71	0.00	0.00	BV	0.1061	55	8.879	12356.59	73858.97	0.15	0.15	VV	0.1673
7	8.493	46.59	505.61	0.00	0.00	VV	0.0921	56	8.882	12926.44	74076.95	0.16	0.16	VV	0.1745
8	8.495	68.36	631.11	0.00	0.00	VV	0.1083	57	8.884	137569.02	73814.29	1.66	1.66	VB	1.8637
9	8.498	87.27	771.69	0.00	0.00	VV	0.1131	58	8.958	47.52	258.37	0.00	0.00	BV	0.1839
10	8.501	142.81	1074.51	0.00	0.00	VV	0.1329	59	8.962	16.14	314.76	0.00	0.00	VB	0.0513
11	8.503	172.67	1511.97	0.00	0.00	VV	0.1142	60	8.964	43.00	243.67	0.00	0.00	BV	0.1764
12	8.506	275.47	2096.31	0.00	0.00	VV	0.1314	61	8.967	30.23	408.93	0.00	0.00	VB	0.0739
13	8.509	392.05	2721.50	0.00	0.00	VV	0.1441	62	8.970	14.32	207.22	0.00	0.00	BB	0.0691
14	8.511	450.27	3376.96	0.01	0.01	VV	0.1333	63	8.975	11.93	226.30	0.00	0.00	BB	0.0527
15	8.514	645.48	4216.42	0.01	0.01	VV	0.1531	64	8.978	18.48	265.82	0.00	0.00	BB	0.0695
16	8.519	1552.63	5894.62	0.02	0.02	VV	0.2634	65	8.980	8.50	159.61	0.00	0.00	BB	0.0533
17	8.522	1010.98	6789.15	0.01	0.01	VV	0.1489	66	8.983	25.92	318.15	0.00	0.00	BB	0.0815
18	8.525	1162.84	7819.38	0.01	0.01	VV	0.1487	67	8.985	7.18	168.91	9e-05	9e-05	BV	0.0425
19	8.527	1327.63	8878.12	0.02	0.02	VV	0.1495	68	8.986	13.73	261.55	0.00	0.00	VB	0.0525
20	8.530	1510.31	10089.78	0.02	0.02	VV	0.1497	69	8.988	56.86	272.05	0.00	0.00	BV	0.2090
21	8.552	21521.76	23881.49	0.26	0.26	VV	0.9012	70	8.993	31.48	272.06	0.00	0.00	VB	0.1157
22	8.554	3916.28	25032.12	0.05	0.05	VV	0.1565	71	8.996	51.16	213.86	0.00	0.00	BV	0.2392
23	8.557	4627.25	25713.31	0.06	0.06	VV	0.1800	72	8.999	10.67	333.89	0.00	0.00	VB	0.0320
24	8.559	4379.62	26019.79	0.05	0.05	VV	0.1683	73	9.004	25.92	269.75	0.00	0.00	BB	0.0961
25	8.562	9901.71	25954.16	0.12	0.12	VV	0.3815	74	9.006	25.22	193.51	0.00	0.00	BB	0.1303
26	8.567	8309.68	25070.62	0.10	0.10	VV	0.3315	75	9.009	20.37	176.06	0.00	0.00	BB	0.1157
27	8.572	1915.96	24033.86	0.02	0.02	VV	0.0797	76	9.012	12.69	261.76	0.00	0.00	BV	0.0485
28	8.575	3368.81	23805.12	0.04	0.04	VV	0.1415	77	9.012	18.72	330.46	0.00	0.00	VB	0.0567
29	8.578	3689.36	23908.68	0.04	0.04	VV	0.1543	78	9.015	16.03	188.59	0.00	0.00	*BB	0.0850
30	8.581	3922.28	24271.94	0.05	0.05	VV	0.1616			8301308.27	3.62e+06	100.00	100.00		
31	8.583	3398.55	24902.34	0.04	0.04	VV	0.1365								
32	8.586	4054.49	25875.04	0.05	0.05	VV	0.1567								
33	8.589	4230.50	27041.78	0.05	0.05	VV	0.1564								
34	8.594	9099.73	29860.21	0.11	0.11	VV	0.3047								
35	8.605	21091.32	35763.97	0.25	0.25	VV	0.5897								
36	8.607	6816.61	36658.49	0.08	0.08	VV	0.1859								
37	8.610	4935.51	36876.89	0.06	0.06	VV	0.1338								
38	8.612	48075.96	36873.03	0.58	0.58	VV	1.3038								
39	8.639	2164.07	19942.86	0.03	0.03	VV	0.1085								
40	8.642	2768.11	20291.31	0.03	0.03	VV	0.1364								
41	8.661	28708.81	32007.54	0.35	0.35	VV	0.8969								
42	8.663	5225.54	33395.14	0.06	0.06	VV	0.1565								
43	8.666	5435.57	34540.10	0.07	0.07	VV	0.1574								
44	8.669	5611.25	35652.13	0.07	0.07	VV	0.1574								
45	8.671	5802.05	36885.86	0.07	0.07	VV	0.1573								
46	8.757	7759165.19	2.05e+06	93.47	93.47	VE	3.7797								
47	8.857	68344.03	66184.49	0.82	0.82	EV	1.0326								
48	8.860	11164.51	69517.84	0.13	0.13	VV	0.1606								

MS Spectra



Certificate of analysis



Date	22/03/2016	Batch	850_s2p1r1
Product name	peptide Contrôle	Catalog #	

Product specifications

AA sequence	C-AEEA-RGEWFWGNLVVSAASFGNHNAGG-OH		
Disulfide bond	0		
Formula	$C_{119}H_{194}N_{36}O_{34}S$		
Appearance	White powder		
Theoretical average weight	2681,89	g/mol	
CAS number			
Source	Synthetic		
Counterion	TFA		
Solubility (recommendation)	50 % of Acetonitrile solution		1 mg/mL

Handling & Storage

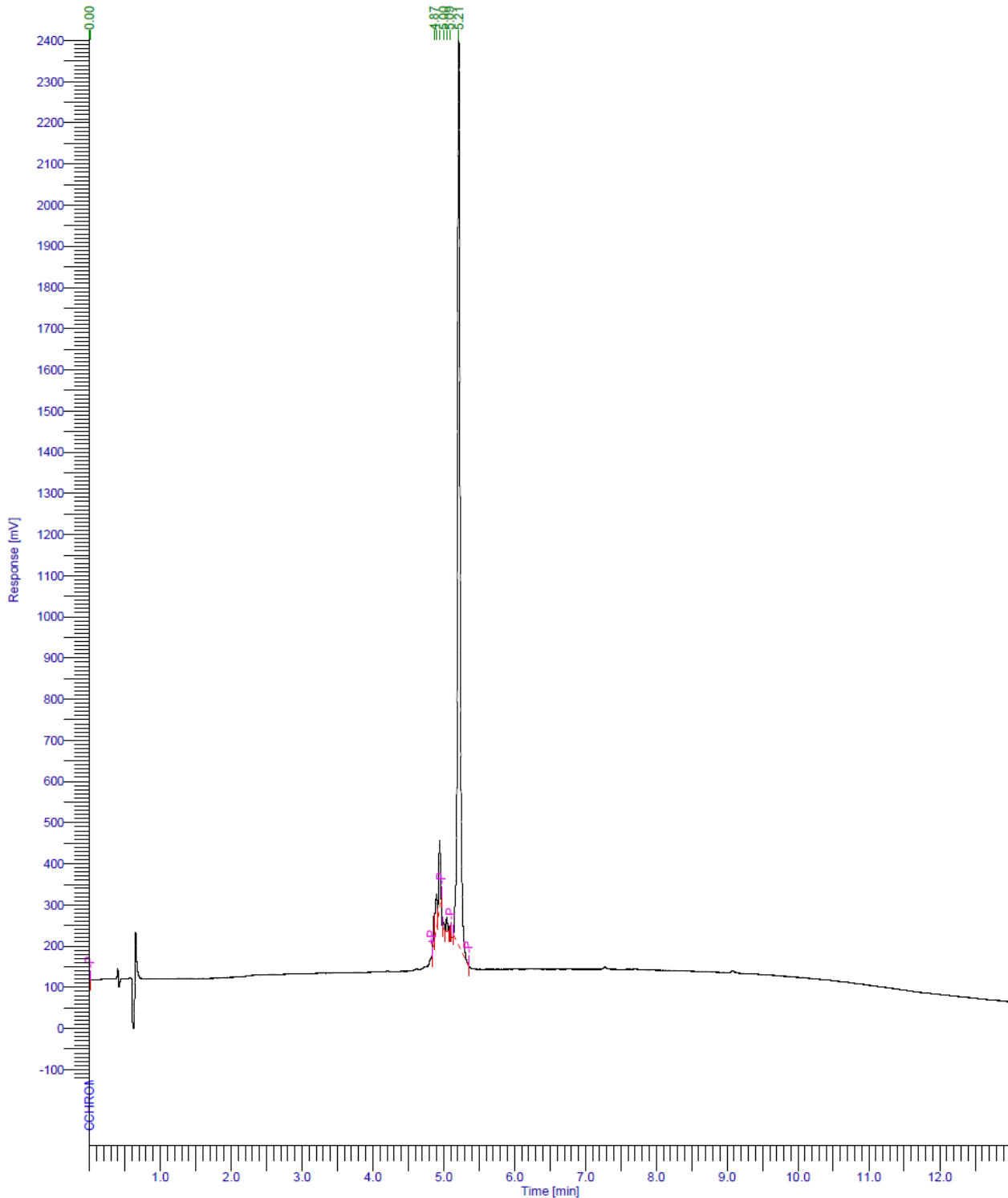
Storage	Shipped at ambient temperature under lyophilized powder. Store at -20°C (-4°F). Do not freeze-thaw. Aliquot sample if required and store at -80°C (-112°F).		
Expiry date	Not defined		
Handling and use restriction	Use with caution. Might be toxic. Product intended for research use only, not for use in diagnostic or therapeutic procedures.		

Analytical results

Observed purity rate	90,49%	Observed monoisotopic mass [M+H] ⁺	2681,17 Da
		Theoretical monoisotopic mass	2680,22 Da

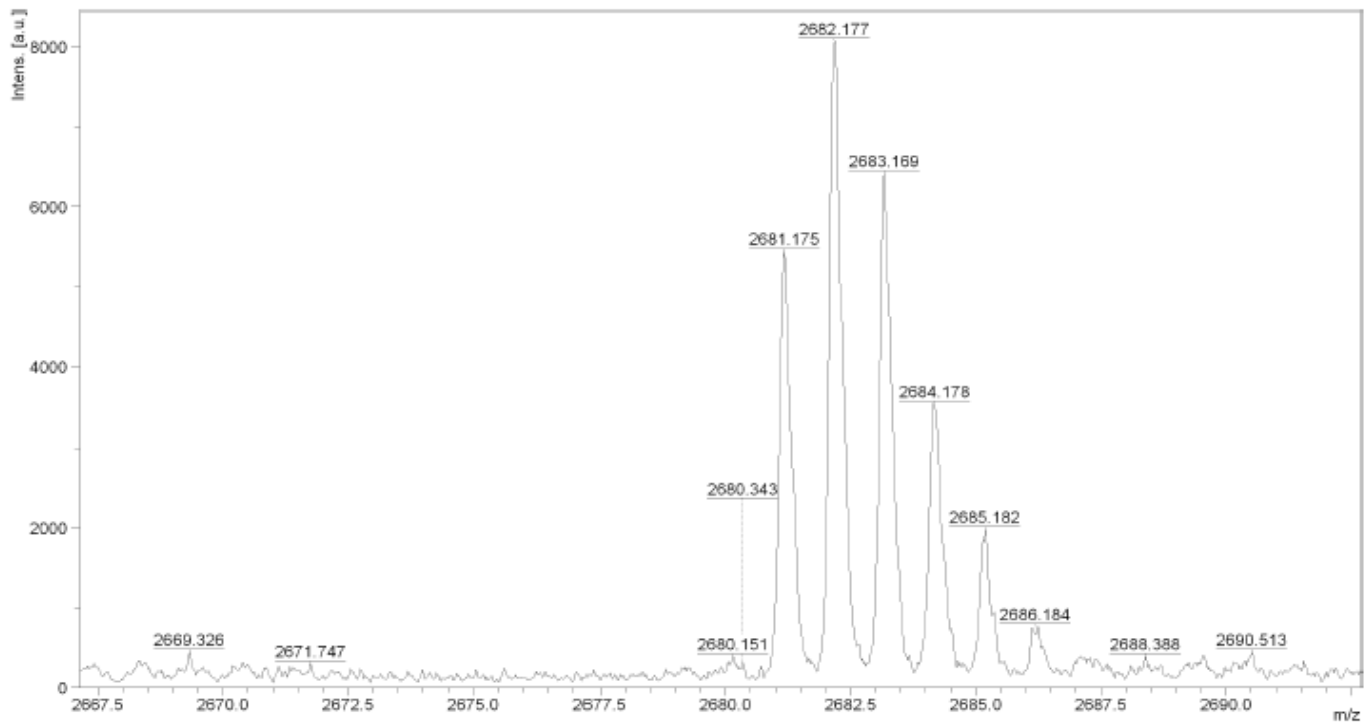
Chromatogram

Sample Name : Sample #: 020 Page 1 of 1
FileName : C:\totalchrom\data\Peptide ceallinjer AEEA fevrier 2016\160314 peptide controle 850 s2p1r1.raw
Date : 3/21/2016 2:42:49 PM
Method : cchromolith 5-95 en 10 min.mth Time of Injection: 3/15/2016 12:11:35 AM
Start Time : 0.00 min End Time : 13.00 min Low Point : -126.41 mAU High Point : 2401.77 mAU
Plot Offset: -126.41 mAU Plot Scale: 2528.2 mAU



Peak #	Time [min]	Area [μ V·s]	Height [μ V]	Area [%]	Norm. Area [%]	BL	Area/Height [s]
-	0.001	0.00	0.00	0.00	0.00		-----
1	0.002	42.54	245.68	0.00	0.00	BV	0.1732
2	0.007	28.29	356.69	0.00	0.00	VB	0.0793
3	4.869	86010.57	65647.89	1.35	1.35	BV	1.3102
4	4.874	7756.18	59133.80	0.12	0.12	VV	0.1312
5	4.898	154870.24	83562.89	2.43	2.43	VV	1.8533
6	4.944	271621.09	161956.69	4.27	4.27	*VB	1.6771
7	5.002	18420.50	16740.93	0.29	0.29	BB	1.1003
8	5.045	49368.87	34018.14	0.78	0.78	BV	1.4513
9	5.085	8310.72	14378.72	0.13	0.13	VV	0.5780
10	5.086	8566.17	14587.51	0.13	0.13	*VB	0.5872
11	5.215	5755579.60	2.20e+06	90.49	90.49	*BB	2.6139
		6360574.77	2.65e+06	100.00	100.00		

MS Spectra



D:\Data\Cermav\2016\Smartox\mars\160315\160315_peptidecontrole_850_s2p1r1_rp\0_113\1

printed: 3/22/2016 1:56:30 PM

Certificate of analysis



Date	21/03/2016	Batch	851_s1p1f1
Product name	Magainin 1-Ccys	Catalog #	

Product specifications

AA sequence	GIGKFLHSAGKFGKAFVGEIMKS-AEEA-C-NH ₂		
Disulfide bond	0		
Formula	C ₁₂₁ H ₁₉₄ N ₃₂ O ₃₁ S ₂		
Appearance	White powder		
Theoretical average weight	2657,16	g/mol	
CAS number			
Source	Synthetic		
Counterion	TFA		
Solubility (recommendation)	10% acetonrile solution		1 mg/mL

Handling & Storage

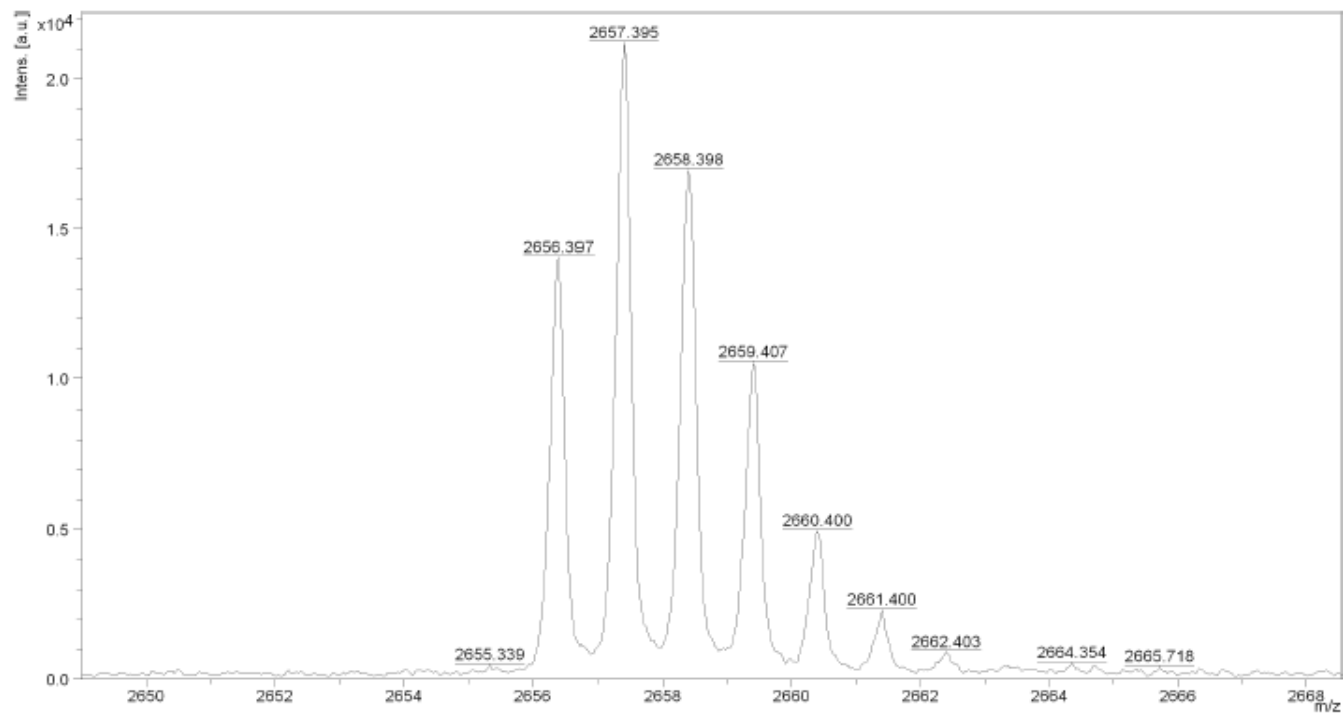
Storage	Shipped at ambient temperature under lyophilized powder. Store at -20°C (-4°F). Do not freeze-thaw. Aliquot sample if required and store at -80°C (-112°F).		
Expiry date	Not defined		
Handling and use restriction	Use with caution. Might be toxic. Product intended for research use only, not for use in diagnostic or therapeutic procedures.		

Analytical results

Observed purity rate	95,61%	Observed monoisotopic mass [M+H] ⁺	2656,39 Da
		Theoretical monoisotopic mass	2655,40 Da

Peak #	Time [min]	Area [μ V-s]	Height [μ V]	Area [%]	Norm. Area [%]	BL	Area/Height [s]
199	7.359	37.65	431.30	0.00	0.00	BV	0.0873
200	7.362	62.26	593.15	0.00	0.00	VV	0.1050
201	7.365	132.78	1181.71	0.00	0.00	VV	0.1124
202	7.367	219.66	1720.05	0.00	0.00	VV	0.1277
203	7.370	322.45	2423.05	0.01	0.01	VV	0.1331
204	7.373	458.22	3113.34	0.01	0.01	VV	0.1472
205	7.375	581.18	3759.34	0.01	0.01	VV	0.1546
206	7.378	628.47	4262.35	0.01	0.01	VV	0.1474
207	7.381	722.46	4530.80	0.01	0.01	VV	0.1595
208	7.383	667.64	4561.89	0.01	0.01	VV	0.1464
209	7.386	774.85	4427.26	0.01	0.01	VV	0.1750
210	7.388	653.02	4062.11	0.01	0.01	VV	0.1608
211	7.391	985.33	3528.49	0.02	0.02	VV	0.2792
212	7.396	476.71	2308.35	0.01	0.01	VV	0.2065
213	7.399	89.65	1576.89	0.00	0.00	VV	0.0569
214	7.401	183.94	1213.24	0.00	0.00	VV	0.1516
215	7.405	88.98	771.10	0.00	0.00	VV	0.1154
216	7.407	47.38	383.29	0.00	0.00	VV	0.1236
217	7.410	27.94	250.60	0.00	0.00	VB	0.1115
218	7.413	22.68	281.60	0.00	0.00	BB	0.0805
219	7.415	16.74	252.52	0.00	0.00	BB	0.0663
220	7.418	20.51	300.09	0.00	0.00	BV	0.0683
221	7.421	48.42	514.08	0.00	0.00	VV	0.0942
222	7.423	97.45	822.22	0.00	0.00	VV	0.1185
223	7.426	122.06	996.43	0.00	0.00	VV	0.1225
224	7.429	189.10	1445.47	0.00	0.00	VV	0.1308
225	7.431	260.02	1923.75	0.00	0.00	VV	0.1352
226	7.434	314.22	2168.52	0.01	0.01	VV	0.1449
227	7.437	380.62	2620.35	0.01	0.01	VV	0.1453
228	7.439	440.35	2809.65	0.01	0.01	VV	0.1567
229	7.442	428.67	2836.71	0.01	0.01	VV	0.1511
230	7.445	441.93	2670.64	0.01	0.01	VV	0.1655
231	7.447	363.58	2458.90	0.01	0.01	VV	0.1479
232	7.449	304.55	2000.89	0.01	0.01	VV	0.1522
233	7.452	108.39	1481.06	0.00	0.00	VV	0.0732
234	7.452	113.68	1357.36	0.00	0.00	VV	0.0838
235	7.454	45.28	776.93	0.00	0.00	VV	0.0583
236	7.455	45.84	672.88	0.00	0.00	VB	0.0681
237	7.458	8.21	151.80	0.00	0.00	BB	0.0541
238	7.460	7.43	151.63	0.00	0.00	BV	0.0490
239	7.460	18.64	318.54	0.00	0.00	VB	0.0585
240	7.482	7.09	184.32	0.00	0.00	BB	0.0384
241	7.484	14.11	191.15	0.00	0.00	BB	0.0738
242	7.487	24.33	286.00	0.00	0.00	BB	0.0851
243	7.490	22.06	315.43	0.00	0.00	BV	0.0699
244	7.493	86.36	687.81	0.00	0.00	VV	0.1256
245	7.495	129.47	1159.81	0.00	0.00	VV	0.1116
246	7.498	199.49	1744.68	0.00	0.00	VV	0.1143
247	7.501	342.53	2635.92	0.01	0.01	VV	0.1299
248	7.504	487.35	3660.54	0.01	0.01	VV	0.1331
249	7.530	20857.84	23066.12	0.36	0.36	VV	0.9043
250	7.538	11995.69	26686.43	0.21	0.21	VV	0.4495
251	7.541	4898.89	27627.31	0.08	0.08	VV	0.1773
252	7.543	3932.89	28745.32	0.07	0.07	VV	0.1368
253	7.641	5583836.78	1.60e+06	95.61	95.61	VB	3.4968
254	7.787	44.38	133.65	0.00	0.00	BB	0.3321
255	7.793	62.63	266.48	0.00	0.00	BB	0.2350
256	7.799	9.21	165.21	0.00	0.00	BB	0.0558
257	7.804	8.21	159.30	0.00	0.00	BB	0.0515
258	7.810	23.68	256.80	0.00	0.00	BB	0.0922
259	7.812	7.74	133.23	0.00	0.00	BB	0.0581
260	7.814	18.66	173.21	0.00	0.00	BB	0.1077
261	7.818	24.98	306.73	0.00	0.00	BV	0.0814
262	7.820	38.38	330.73	0.00	0.00	VB	0.1161
263	7.823	33.27	345.67	0.00	0.00	BV	0.0962
264	7.826	24.46	242.86	0.00	0.00	VB	0.1007
265	7.828	13.35	179.63	0.00	0.00	BB	0.0743
266	7.831	25.25	331.23	0.00	0.00	BB	0.0762
267	7.834	20.37	229.47	0.00	0.00	BB	0.0888
268	7.836	3.72	86.70	6e-05	6e-05	BV	0.0429
269	7.836	7.44	187.96	0.00	0.00	VB	0.0396
270	7.839	29.06	310.31	0.00	0.00	BV	0.0936
271	7.842	23.68	282.79	0.00	0.00	VB	0.0837
272	7.844	27.16	287.98	0.00	0.00	BB	0.0943
273	7.847	34.04	353.19	0.00	0.00	BV	0.0964

MS Spectra



D:\Data\Cermav\2016\Smartox\mars\160308\160308_Magainin_cCys_851_S1P1F1_RP10_F24\1

printed: 3/22/2016 1:58:22 PM

Certificate of analysis



Date	21/03/2016	Batch	852_s1p1f2
Product name	peptide PGQ	Catalog #	

Product specifications

AA sequence	GVLSNVIGYLKKGALNAVLKQ-AEEA-C-NH ₂		
Disulfide bond	0		
Formula	C ₁₂₁ H ₂₁₁ N ₃₃ O ₃₄ S		
Appearance	White powder		
Theoretical average weight	2704,23	g/mol	
CAS number			
Source	Synthetic		
Counterion	TFA		
Solubility (recommendation)	Water		1 mg/mL

Handling & Storage

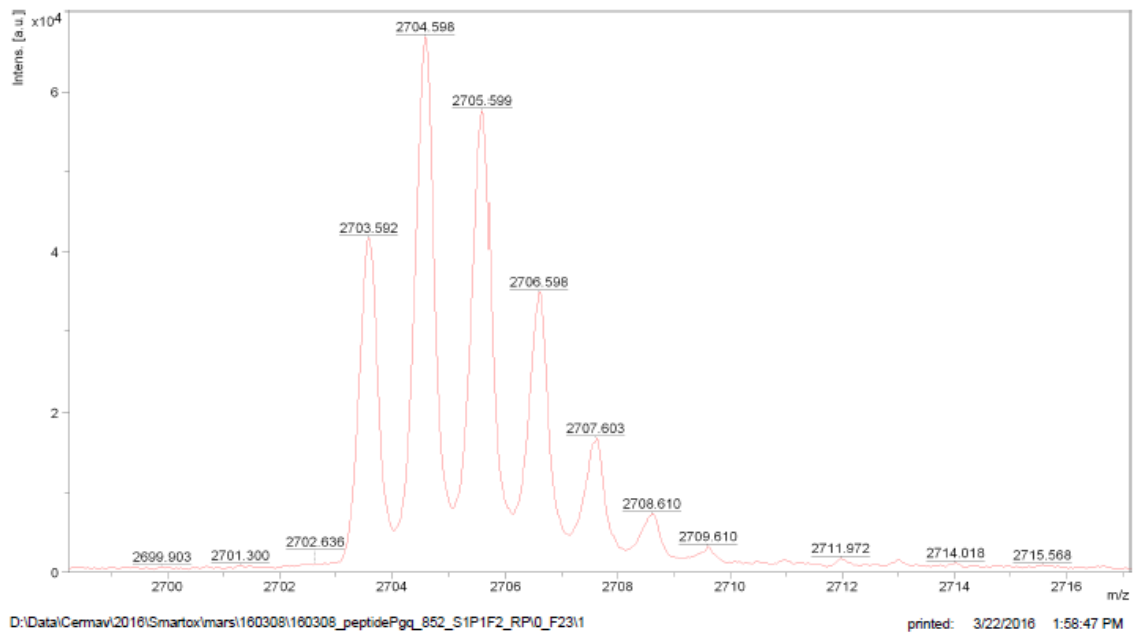
Storage	Shipped at ambient temperature under lyophilized powder. Store at -20°C (-4°F). Do not freeze-thaw. Aliquot sample if required and store at -80°C (-112°F).		
Expiry date	Not defined		
Handling and use restriction	Use with caution. Might be toxic. Product intended for research use only, not for use in diagnostic or therapeutic procedures.		

Analytical results

Observed purity rate	97,92%	Observed monoisotopic mass [M+H] ⁺	2703,59 Da
		Theoretical monoisotopic mass	2702,55 Da

Peak #	Time [min]	Area [μ V-s]	Height [μ V]	Area [%]	Norm. Area [%]	BL	Area/Height [s]	Peak #	Time [min]	Area [μ V-s]	Height [μ V]	Area [%]	Norm. Area [%]	BL	Area/Height [s]
-	0.001	0.00	0.00	0.00	0.00		-----	49	10.829	24.04	263.16	0.00	0.00	BV	0.0914
1	0.003	26.52	301.71	0.00	0.00	BV	0.0879	50	10.832	26.03	335.05	0.00	0.00	VB	0.0777
2	0.005	29.05	300.47	0.00	0.00	VB	0.0967	51	10.837	24.58	307.76	0.00	0.00	BV	0.0799
3	0.008	24.28	289.71	0.00	0.00	BV	0.0838	52	10.840	30.64	345.61	0.00	0.00	VB	0.0886
4	0.011	22.94	211.76	0.00	0.00	VB	0.1083	53	10.843	9.97	170.24	0.00	0.00	BV	0.0586
5	0.014	28.98	347.00	0.00	0.00	BV	0.0835	54	10.846	29.15	328.11	0.00	0.00	VB	0.0888
6	0.016	22.64	288.75	0.00	0.00	VB	0.0784	55	10.848	136.69	337.24	0.02	0.02	BV	0.4053
7	0.019	21.52	304.84	0.00	0.00	BB	0.0706	56	10.867	26.36	285.40	0.00	0.00	VB	0.0923
8	0.022	22.65	211.65	0.00	0.00	BV	0.1070	57	10.870	34.13	304.59	0.00	0.00	BV	0.1120
9	0.024	16.55	272.74	0.00	0.00	VV	0.0607	58	10.872	20.12	300.86	0.00	0.00	VB	0.0669
10	0.027	18.71	212.36	0.00	0.00	VB	0.0881	59	10.875	52.51	312.16	0.01	0.01	BV	0.1682
11	10.520	19.13	255.53	0.00	0.00	BB	0.0749	60	10.880	22.81	265.18	0.00	0.00	VB	0.0860
12	10.522	23.27	169.37	0.00	0.00	BV	0.1374	61	10.883	17.27	225.33	0.00	0.00	BB	0.0767
13	10.526	15.88	243.23	0.00	0.00	VB	0.0653	62	10.885	25.49	158.79	0.00	0.00	BV	0.1606
14	10.528	25.54	305.91	0.00	0.00	BB	0.0835	63	10.887	21.14	160.78	0.00	0.00	VV	0.1315
15	10.531	16.48	263.72	0.00	0.00	BV	0.0625	64	10.891	30.08	353.87	0.00	0.00	VB	0.0850
16	10.534	22.87	232.41	0.00	0.00	VV	0.0984	65	10.894	37.96	366.72	0.01	0.01	BV	0.1035
17	10.536	26.20	281.86	0.00	0.00	VV	0.0929	66	10.896	106.50	405.85	0.01	0.01	VV	0.2624
18	10.538	23.62	159.49	0.00	0.00	VB	0.1481	67	10.902	78.88	641.81	0.01	0.01	VV	0.1229
19	10.542	26.52	341.29	0.00	0.00	BV	0.0777	68	10.904	90.73	712.83	0.01	0.01	VV	0.1273
20	10.544	31.06	340.05	0.00	0.00	VV	0.0913	69	10.907	123.82	952.87	0.02	0.02	VV	0.1299
21	10.547	29.26	292.68	0.00	0.00	VV	0.1000	70	10.910	156.64	1079.11	0.02	0.02	VV	0.1452
22	10.550	42.07	413.02	0.01	0.01	VV	0.1019	71	10.912	181.51	1279.32	0.02	0.02	VV	0.1419
23	10.552	38.50	376.56	0.01	0.01	VV	0.1022	72	10.915	204.72	1426.92	0.03	0.03	VV	0.1435
24	10.555	62.27	409.42	0.01	0.01	VV	0.1521	73	10.917	235.91	1479.75	0.03	0.03	VV	0.1594
25	10.558	32.11	364.78	0.00	0.00	VV	0.0880	74	10.920	273.92	1858.63	0.04	0.04	VV	0.1474
26	10.560	41.41	404.20	0.01	0.01	VV	0.1024	75	10.922	281.59	1868.97	0.04	0.04	VV	0.1507
27	10.563	36.64	364.94	0.01	0.01	VV	0.1004	76	10.926	352.73	2232.73	0.05	0.05	VV	0.1580
28	10.566	37.36	416.20	0.01	0.01	VV	0.0898	77	10.928	317.93	2428.64	0.04	0.04	VV	0.1309
29	10.568	44.15	421.07	0.01	0.01	VV	0.1048	78	10.931	567.64	2526.52	0.08	0.08	VV	0.2247
30	10.571	54.39	527.65	0.01	0.01	VV	0.1031	79	10.934	310.00	2632.88	0.04	0.04	VV	0.1177
31	10.574	67.34	543.85	0.01	0.01	VV	0.1238	80	10.936	390.51	2838.37	0.05	0.05	VV	0.1376
32	10.576	61.73	545.19	0.01	0.01	VV	0.1132	81	10.939	408.08	2942.89	0.06	0.06	VV	0.1387
33	10.578	72.76	450.51	0.01	0.01	VV	0.1615	82	10.942	560.08	3054.82	0.08	0.08	VV	0.1833
34	10.582	96.41	772.89	0.01	0.01	VV	0.1247	83	10.944	448.63	3033.79	0.06	0.06	VV	0.1479
35	10.584	140.43	1023.12	0.02	0.02	VV	0.1373	84	10.947	474.21	3067.70	0.07	0.07	VV	0.1546
36	10.587	169.01	1280.76	0.02	0.02	VV	0.1320	85	10.950	409.57	3020.90	0.06	0.06	VV	0.1356
37	10.590	226.00	1697.16	0.03	0.03	VV	0.1332	86	10.952	425.28	2909.80	0.06	0.06	VV	0.1462
38	10.593	269.07	2109.73	0.04	0.04	VV	0.1275	87	10.954	1651.34	2754.66	0.23	0.23	VV	0.5995
39	10.595	385.55	2803.13	0.05	0.05	VV	0.1375	88	10.965	324.40	2294.14	0.04	0.04	VV	0.1414
40	10.659	713376.20	177068.23	97.92	97.92	VE	4.0288	89	10.968	1416.51	2199.07	0.19	0.19	VV	0.6441
41	10.778	480.16	541.27	0.07	0.07	EV	0.8871	90	10.981	200.95	1192.57	0.03	0.03	VV	0.1685
42	10.784	52.68	487.43	0.01	0.01	VB	0.1081	91	10.984	457.77	1108.28	0.06	0.06	VB	0.4130
43	10.789	72.49	350.17	0.01	0.01	BV	0.2070	92	10.998	77.21	366.21	0.01	0.01	BB	0.2108
44	10.795	126.34	335.42	0.02	0.02	VB	0.3767	93	11.003	33.23	397.56	0.00	0.00	BV	0.0836
45	10.805	92.42	355.28	0.01	0.01	BB	0.2601	94	11.006	124.41	388.92	0.02	0.02	VB	0.3199
46	10.813	25.22	318.08	0.00	0.00	BB	0.0793	95	11.019	31.35	261.11	0.00	0.00	BV	0.1201
47	10.816	34.37	379.36	0.00	0.00	BB	0.0906	96	11.024	44.46	289.73	0.01	0.01	VB	0.1535
48	10.819	91.53	314.50	0.01	0.01	BB	0.2910	97	11.030	54.36	333.48	0.01	0.01	BV	0.1630
								98	11.035	18.22	232.92	0.00	0.00	VB	0.0782
								99	11.038	33.54	335.20	0.00	0.00	BV	0.1000
								100	11.040	30.71	345.51	0.00	0.00	VB	0.0889
								101	11.043	21.65	279.85	0.00	0.00	BV	0.0774
								102	11.045	33.30	347.73	0.00	0.00	VB	0.0958
								103	11.051	29.02	369.13	0.00	0.00	BB	0.0786
								104	11.054	28.70	373.50	0.00	0.00	BV	0.0768
								105	11.056	31.06	291.98	0.00	0.00	VV	0.1064
								106	11.059	25.19	342.14	0.00	0.00	VB	0.0736
								107	11.062	43.11	273.54	0.01	0.01	BB	0.1576
								108	11.067	10.15	148.59	0.00	0.00	BV	0.0683
								109	11.070	13.56	249.56	0.00	0.00	VB	0.0543
								110	11.071	17.04	146.92	0.00	0.00	BB	0.1160
								111	11.074	16.24	122.07	0.00	0.00	BB	0.1330
								112	11.077	14.82	176.29	0.00	0.00	BB	0.0841
								113	11.083	25.45	308.59	0.00	0.00	BV	0.0825
								114	11.086	15.50	173.15	0.00	0.00	*VB	0.0895
										728513.35	264018.78	100.00	100.00		

MS Spectra



Certificate of analysis



Date	22/03/2016	Batch	853_s1p1r2
Product name	Leucocin A 24	Catalog #	

Product specifications

AA sequence	C-AEEA-SVNWGEAFSAGVHRLANGNGFW-OH		
Disulfide bond	0		
Formula	$C_{119}H_{170}N_{36}O_{34}S$		
Appearance	White powder		
Theoretical average weight	2681,89	g/mol	
CAS number			
Source	Synthetic		
Counterion	TFA		
Solubility (recommendation)	50% of Acetonitrile solution		1 mg/mL

Handling & Storage

Storage	Shipped at ambient temperature under lyophilized powder. Store at -20°C (-4°F). Do not freeze-thaw. Aliquot sample if required and store at -80°C (-112°F).		
Expiry date	Not defined		
Handling and use restriction	Use with caution. Might be toxic. Product intended for research use only, not for use in diagnostic or therapeutic procedures.		

Analytical results

Observed purity rate	90,34%	Observed monoisotopic mass [M+H ⁺] ⁺	2681,12 Da
		Theoretical monoisotopic mass	2680,22 Da

Peak #	Time [min]	Area [$\mu\text{V}\cdot\text{s}$]	Height [μV]	Area [%]	Norm. Area [%]	BL	Area/Height [s]
-	0.001	0.00	0.00	0.00	0.00		-----
1	0.002	13.20	202.92	0.00	0.00	BB	0.0650
2	0.004	24.09	271.87	0.00	0.00	BV	0.0886
3	0.007	26.34	302.68	0.00	0.00	VB	0.0870
4	0.010	17.32	234.24	0.00	0.00	*BB	0.0739
5	6.270	170379.05	81098.26	1.60	1.60	*BB	2.1009
6	6.426	195125.07	117045.40	1.84	1.84	*BB	1.6671
7	6.498	304319.96	145871.10	2.87	2.87	*BB	2.0862
8	6.594	355984.87	202441.13	3.35	3.35	*BB	1.7585
9	6.708	9591283.16	2.79e+06	90.34	90.34	*BB	3.4412
		10617173.06	3.33e+06	100.00	100.00		

MS Spectra

